

# Onboard Fuzzy Logic Approach to Active Fire Detection in Brazilian Amazon Forest

**BRUNA E. Z. LEAL**  
**ANDRE R. HIRAKAWA**  
University of São Paulo  
São Paulo, Brazil

**THIAGO D. PEREIRA**  
Brazilian National Institute for Space Research (INPE)  
São Paulo, Brazil

**In Brazil, almost all fires are caused by human activities, and for very different reasons: cleaning pastures, preparation for planting, removal of excess undergrowth, hand harvesting of cane sugar, vandalism, etc. Identifying fire occurrence promptly can assist and minimize the negative impact on the affected area. This article presents an onboard fuzzy logic approach for identifying and detecting active fire spots in the Brazilian Amazon forest considering the separability of fire spectral characteristics.**

Manuscript received October 13, 2014; revised May 19, 2015; released for publication October 19, 2015.

DOI. No. 10.1109/TAES.2015.140766.

Refereeing of this contribution was handled by H. Kwon.

Authors' addresses: B. E. Z. Leal and A. R. Hirakawa, University of São Paulo, Laboratório de Automação Agrícola, Escola Politécnica da USP, Av. Prof. Luciano Gualberto, travessa 3, no. 158, sala C2-56, Sao Paulo, Sao Paulo 05508-900, Brazil; T. D. Pereira, Av. Dos Astronautas, 1758 Jardim da Granja, São José dos Campos, São Paulo 12227-010, Brazil. Corresponding author is B. E. Z. Leal, E-mail: (brunaezleal@gmail.com).

0018-9251/16/\$26.00 © 2016 IEEE

## I. INTRODUCTION

Fire spots occur throughout the world, with local impacts on land use, productivity, evapotranspiration, biodiversity, etc., and global and regional impacts related to biochemical, hydrological, and atmospheric processes [1]. Fire spots are caused mainly by factors such as climate, vegetation conditions, and human activities, which are intrinsically related [2]. Fires occurrences in the Amazon forest are mainly concentrated in the so-called arc of deforestation, which corresponds to the area of agricultural expansion. The cultural practice of burning is related to the traditional method of clearing land for introduction and/or maintenance of pastures and agricultural fields [3].

Several initiatives have been taken to improve the mechanisms for detection of fires [4, 5]. Researches on this topic are related to remote sensing analysis of satellite images [6]. The satellite images show information that, when processed by central monitoring systems, assists in the identification of fires in uninhabited areas.

For monitoring and modeling of natural phenomena, the use of satellite images, especially from National Oceanic and Atmospheric Administration (NOAA) satellites, aiming at large-scale environmental monitoring, is of great importance [7]. Satellite data have been widely used for the process of detection and monitoring of fires, especially in areas of environmental preservation, tropical forests, and savannas [8–11], the forests of the Northern Hemisphere [12, 13], as well as the forests of the American continent [14] and Mediterranean areas [15]. The main instrument of the satellite, directly related to remote sensing, is the multispectral sensor. For remote sensing, the fundamentals are based on electromagnetic radiation and its interaction with matter properties [16]. This radiation is received by the sensors in analogue or digital format and used for the processing of relevant information in pattern recognition processes [16]. The techniques of multispectral image analysis were developed to explore the spectral response of various characteristics in different bands of the electromagnetic spectrum. The different characteristics tend to have different responses in various bands.

The spectral behavior, also called spectral characteristic of targets, is related to the process of interaction between the objects and terrestrial features with incident electromagnetic radiation (EMR) [17]. By comparing the response pattern of the different characteristics of the element, one can distinguish it from other elements, which would not be possible if only the comparison of the wavelength was considered [17]. The satellite sensors are sensitive to these differences (in accordance with each spectrum). For classification of targets, the algorithms generally use similar procedures and can be separated into two categories: fixed limits (thresholds) or contextual methods [18]. The fixed limits algorithms are generally based on the absolute updated values and consider a single pixel at a time, while the

contextual methods are based on statistics compiled by the pixels in relation to their neighbors [19]. Among the main projects, one can highlight the Bi-spectral Infra-Red Detection (BIRD) project developed by Deutschen Zentrums für Luft- und Raumfahrt (DLR; German Aerospace Center) [20], the FOCUS project [21] presented jointly by DLR and NASA, and the FUEGO project [38] developed by the European Space Agency (ESA) led jointly with Ingeniería y Servicios Aeroespaciales (INSA). The BIRD project realizes the autonomous identification of fire through an artificial neural network onboard the satellite. This paper presents an approach for using a fuzzy system for the process of identifying fire spots suitable for an onboard algorithm to be embedded in the satellite as an alternative to the threshold method proposed by Setzer et al. [25].

## II. THE PATTERN RECOGNITION PROCESS

The precision and accuracy of a fire detection algorithm are measured in terms of levels of commission or omission errors in the location of the detected fire spot that should be well defined and documented [22]. The units of a pattern recognition system and their assignments are described by the following steps [23]:

- 1) Acquisition of patterns, which can be accomplished in several ways such as acquisition of signals or images, acquisition of data collections, etc.
- 2) Feature extraction in the form of measures, primitive data extraction, etc.
- 3) Preprocessing—in some cases, the values of the features are not directly classified, so a preprocessing stage must be performed for the classification process.
- 4) Classification, regression, or descriptions, which are considered to be the core of a pattern recognition system.
- 5) Postprocessing—in some cases, the outputs generated by the classification unit are not directly used, and they may require some decoding operation so that the data can be interpreted.

Selecting patterns in an image is an inherently human activity, where the process of pattern recognition is performed from a selection of the information that is considered significant, according to an expert. From the extraction of this information, a computational classification can be performed.

A fuzzy classifier involves a probabilistic approach and is a robust technique for classification of problems, because it reiterates rules of an expert system and explores similarities between spectral signatures of the same class [24]. Due to these factors, the use of a fuzzy classifier in a pattern recognition system favors the inclusion of human reasoning in feature selection and classification for extracting this information by means of rules in the fuzzy system.

## III. THE SETZER ALGORITHM

One of the main problems in identifying fire is the definition of a spectral characteristic that best represents the pixels of fire. The spectral indices currently considered were selected due to their own empirical characteristics [25]. According to Setzer et al. [26], the National Institute for Space Research (INPE) algorithm for identification of fire used in the Advanced Very High Resolution Radiometer (AVHRR) NOAA series of satellites (in use until the end of 2012) remained essentially the same for 25 y. The analysis of pixels is done from their natural values (digital numbers [DNs]) without converting these values for temperature or reflectance. The thresholds used to classify fire pixels are obtained empirically, requiring only a few annual adjustments to account for the sensor's degradation.

These values are affected by the spectral response of the object, the spatial resolution of the land surface, the size of objects in the scene, neighbors of the objects, and other features. DN's are represented by a linear function of temperature (for the thermal channel) or percentage of the albedo (the visible channels). The temperature of the infrared thermal images, which starts at  $-50^{\circ}\text{C}$ , corresponds to DN equal to 0, and increases by 0.1 degrees Celsius per DN. Therefore, for any DN, the corresponding temperature in degrees Celsius is given by:

$$\text{temperature } (^{\circ}\text{C}) = (\text{count} \times 0.1) - 50 \quad (1)$$

The conversion of values acquired by the sensors in DN's is required since electromagnetic waves reaching the sensor are continuous radiation flows [27] and must be stored so they can be analyzed later. The number of DN's in a digital image is determined by the number of available bits [28]. Additionally, one should take into account the different spectral bands of a sensor to perform data capture at different exposure times, which results in a necessary radiometric correction of the data for image analysis. This is very important for the development of algorithms, which require consistency in different scenes collected in varying weather conditions and in different geographic locations [24]. The method for detection of fires employed by INPE is based on an unsupervised clustering algorithm that selects the pixels according to the rule:

**RULE 1** *If the radiometric temperature from the AVHRR sensor exceeds  $46^{\circ}\text{C}$ , then the occurrence of fire exists at that pixel [29]. Moreover, detections made above the oceans are eliminated [26].*

The method of the saturation limit (or threshold) of the mid-infrared channel is based on the knowledge that a pixel of fire reaches a saturation value when it is fully or partially occupied by the fire, depending on the size or temperature of the fire [29].

In simple cases, the images tend to have a bimodal histogram that can be segmented in two different regions separated by the pixels having values higher than a preset value belonging to the scene and the pixels having the

lower limit [30]. When there is no knowledge about the spectral characteristics and phenomenology of the element, other techniques, such as data mining, statistical analysis, and histograms, can be taken into consideration for the acquisition of this knowledge. According to De Souza et al. [31], the regional coverage of the satellite data, the angles of the target, the observation time, and spatial resolution of the sensor all affect the process for detecting fires. In the range between  $3 \mu\text{m}$  and  $5 \mu\text{m}$ , radiation is either reflected or emitted [32]. Thus, the region around  $3.7 \mu\text{m}$  of the mid-infrared band from the AVHRR sensor is particularly complex because it contains as much information from the electromagnetic spectrum as reflected radiation [33].

Nevertheless, it is still regarded as the best spectral range to be used in this sensor for detection of fires [34], due to the fact that the imaging of fire in this range makes possible the detection of the fronts of fire and hot spots. As regards the thermal infrared spectral range, including wavelengths between  $7$  and  $15 \mu\text{m}$ , emissions tend to increase after the occurrence of fire, due to the increased soil temperature, caused by the reduction of evapotranspiration and the increase in the absorption coefficient of the surface.

#### IV. FUZZY LOGIC APPROACH

As a case of study, this paper presents a fuzzy logic approach for fire detection using AVHRR images from the NOAA-16 satellite. Images from this satellite were collected at INPE Reception Station located at the city of Cachoeira Paulista, Sao Paulo State, Brazil. The study area refers to the arc of deforestation in the Amazon, considered due to the high environmental impact in this region. According to Liu [22], sensor data do not give accurate estimates of the state-variable values being monitored and controlled, especially when noise and disturbances inside or outside the system prevent accurate observations of its state and not all the parameters representing the dynamics of the system are known.

In the system, two input variables are considered: PixelValue, which represents the original pixel value in DN format, from the mid-infrared band of the AVHRR sensor; and HousekeepingDiagnosticParameter, which represents an estimative condition of the overall system. The housekeeping telemetry is considered to deal with the problem of reliability of the data generated by the sensor at the time they were being recorded. The Gaussian function that represents PixelValue variables is defined as

$$f(x, \sigma, c) = \exp((-0.5(x - c)^2/\sigma^2) \quad (2)$$

This function depends on two parameters:  $\sigma$  and  $c$ , listed in order in the vector [sig c] of the following relation

$$y = \text{gaussmf}(x, [\text{sig } c]) \quad (3)$$

The HousekeepingDiagnosticParameter variable is defined by a triangular function. The triangular curve is a function of a vector  $x$  and depends on three scalar parameters  $a$ ,  $b$ ,

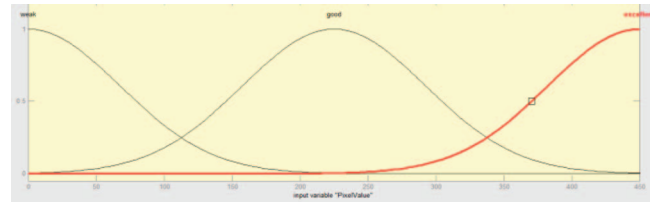


Fig. 1. Membership function plot for PixelValue input variable.

and  $c$ , as given by

$$f(x; a, b, c) = \{(0, x \leq a \text{ or } c \leq x \\ (x - a)/(b - a), a \leq x \leq b \\ (c - x)/(c - b), b \leq x \leq c)\} \quad (4)$$

The parameters  $a$  and  $c$  are located at the base of the triangle, and the parameter  $b$  is located at the apex. They are defined as

$$y = \text{trimf}(x, [a \ b \ c]) \quad (5)$$

Fig. 1 shows the Membership function, which denotes the membership of an object in a class, for the PixelValue input variable. This variable represents the raw sensor data acquired from channel 3A as defined by Setzer et al. [25]. A pixel is considered as a fire pixel when its value is between [0 to 450]. Due to the intrinsic nature of this approach, to define this range empirically, a Gaussian function was selected to represent these variables. The semantic values defined to represent how a pixel value can be classified were:

1) Weak—This means that the pixel value is weak, or not intense. Its range is between [0 to 450], according to Setzer's algorithm, and its parameters for Gaussian function are  $\text{sig } c = [67.5 \ 0]$ , where  $b = 67.5$ , and  $c = 0$ , as represented in

$$y = \text{gaussmf}(x, [67.5 \ 0]) \quad (6)$$

2) Good—This means that the pixel value is reasonable, or neither intense nor weak. Its range is also between [0 to 450]. Its parameters for Gaussian function are  $[67.5 \ 225]$ , where  $b = 67.5$ , and  $c = 225$ , as represented in

$$y = \text{gaussmf}(x, [67.5 \ 225]) \quad (7)$$

3) Excellent—This means that the pixel value is very high or intense. Its range is also between [0 to 450], and its parameters for Gaussian function are  $[67.5 \ 450]$ , where  $b = 67.5$ , and  $c = 450$ , as represented in

$$y = \text{gaussmf}(x, [67.5 \ 450]) \quad (8)$$

Fig. 2 shows the Membership function for the HousekeepingDiagnosticParameter input variable. This variable represents the general state of the onboard computer, where data are loaded. It is important in a real-time system to monitor the status of the high-priority parameter, especially due to the fact that the computer is

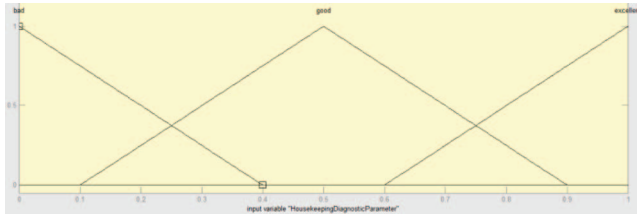


Fig. 2. Membership function plot for HousekeepingDiagnosticParameter input variable.

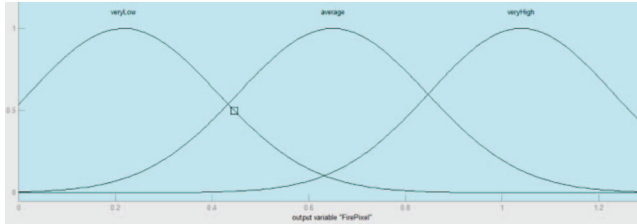


Fig. 3. Membership function plot for FirePixel output variable.

running in a critical environment, full of external hazardous threats. The semantic values defined to represent how the housekeeping and diagnostic parameters onboard the satellite can be classified are:

1) Bad—This means that, in general, the satellite condition indicates that it has some problems that may be critical to its normal operation, and processing data in such conditions may affect the final results. Its range is between [0 1], and its parameters for triangular function are  $[-0.4 \ 0 \ 0.4]$ , where  $a = -0.4$ ,  $b = 0$ , and  $c = 0.4$ , represented in

$$y = \text{trimf}(x, [-0.4 \ 0 \ 0.4]) \quad (9)$$

2) Good—This means that, in general, the satellite condition indicates that it has some problems, but it is in a safe state to perform its normal operation, and processing data in such conditions may not affect the final results. Its range is between [0 1], and its parameters for triangular function are  $[0.1 \ 0.5 \ 0.9]$ , where  $a = 0.1$ ,  $b = 0.5$ , and  $c = 0.9$ , represented in

$$y = \text{trimf}(x, [0.1 \ 0.5 \ 0.9]) \quad (10)$$

3) Excellent—This means that, in general, satellite condition indicates that it does not have any problem and is in a perfect state to perform its normal operation, and processing data in such conditions will not affect the final results. Its range is between [0 1], and its parameters for triangular function are  $[0.6 \ 1 \ 1.4]$ , where  $a = 0.6$ ,  $b = 1$ , and  $c = 1.4$ , represented in

$$y = \text{trimf}(x, [0.6 \ 1 \ 1.4]) \quad (11)$$

The output of this fuzzy logic system is the FirePixel value as shown in Fig. 3.

The fuzzy output variables are defuzzified to yield a crisp number for output. Semantic representation for this value is as follows.

TABLE I  
Bandwidth for the Channels on NOAA/AVHRR Sensor

| Channels             | Spectral Bands ( $\mu\text{m}$ ) |
|----------------------|----------------------------------|
| 1 (Visible)          | 0.560–0.68                       |
| 2 (Near Infrared)    | 0.725–1.10                       |
| 3B (Mid-Infrared)    | 3.550–3.93                       |
| 4 (Thermal Infrared) | 10.300–11.3                      |
| 5 (Thermal Infrared) | 11.500–12.5                      |

TABLE II  
Samples of Each Channel of AVHRR/NOAA Sensor

| Channel 1 | Channel 2 | Channel 3 | Channel 4 | Channel 5 |
|-----------|-----------|-----------|-----------|-----------|
| 245.65    | 238.45    | 298.95    | 267.55    | 268.55    |
| 248.05    | 240.85    | 296.95    | 267.65    | 268.55    |
| 243.85    | 236.95    | 298.45    | 267.35    | 268.45    |
| 243.55    | 236.55    | 299.45    | 267.35    | 268.35    |
| 243.85    | 236.95    | 298.95    | 267.25    | 268.35    |
| 243.55    | 236.65    | 298.85    | 267.15    | 268.15    |
| 241.75    | 234.95    | 300.15    | 267.05    | 268.05    |
| 244.65    | 237.65    | 300.15    | 267.05    | 268.15    |
| 245.75    | 238.75    | 299.55    | 267.15    | 268.15    |
| 243.05    | 236.25    | 299.55    | 267.05    | 268.05    |
| 239.65    | 233.05    | 301.15    | 266.75    | 267.95    |
| 237.95    | 231.45    | 302.75    | 266.65    | 267.85    |
| 238.25    | 231.75    | 302.75    | 266.85    | 267.95    |
| 238.95    | 232.35    | 302.25    | 266.95    | 268.05    |
| 239.55    | 232.95    | 301.45    | 266.95    | 268.15    |
| 238.55    | 232.05    | 302.05    | 266.85    | 267.95    |
| 238.05    | 231.65    | 302.55    | 266.65    | 267.75    |
| 237.65    | 231.25    | 302.75    | 266.55    | 267.65    |
| 237.55    | 231.15    | 302.95    | 266.45    | 267.65    |
| 237.35    | 231.05    | 303.05    | 266.45    | 267.75    |
| 237.35    | 231.05    | 302.85    | 266.45    | 267.65    |

1) Very low—This indicates that the chances of the output being a fire pixel are very low. Its range is between [0 1.3], and its parameters for Gaussian function are  $[0.195 \ 0.2171]$ , where  $b = 0.195$  and  $c = 0.2171$ , as represented in

$$y = \text{gaussmf}(x, [0.195 \ 0.2171]) \quad (12)$$

2) Average—This indicates that the chances of the output being a fire pixel are medium or average. Its range is between [0 1.3], and its parameters for Gaussian function are  $[0.195 \ 0.65]$ , where  $b = 0.195$  and  $c = 0.65$ , as represented in

$$y = \text{gaussmf}(x, [0.195 \ 0.65]) \quad (13)$$

3) Very high—This indicates that the chances of the output being a fire pixel are very high. Its range is between [0 1.3], and its parameters for Gaussian function are  $[0.1909 \ 1.04]$ , where  $b = 0.1909$  and  $c = 1.04$ , as represented in

$$y = \text{gaussmf}(x, [0.1909 \ 1.04]) \quad (14)$$

AVHRR channels are distributed as presented in Table I. Table II presents samples of each channel from the AVHRR NOAA sensor. Those data are already preprocessed and calibrated. As can be noticed from data

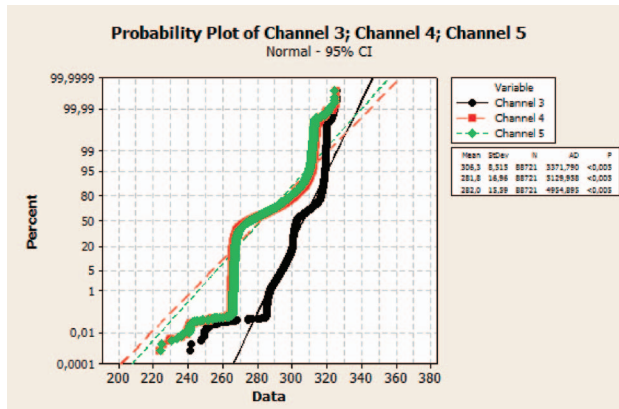


Fig. 4. Plotting sample of each channel.

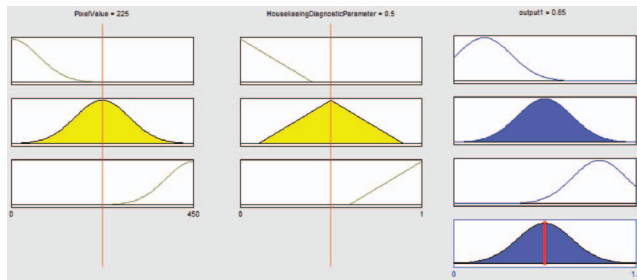


Fig. 5. Rule viewer for proposed fuzzy system for onboard fire identification process.

analysis of Table II, channels 1 and 2 and channels 4 and 5 are intrinsically related, and applying these data to a pattern recognition algorithm may cause the problem of not converging to a correct interpretation. Fig. 4 shows the probability plot of channels 3, 4, and 5, and as can be noticed, channels 4 and 5 are not suitable to distinguish the patterns from the data since they have poor separability between each other.

Fig. 5 shows a simulation process for input values, respectively:

- 1) PixelValue = 280;
- 2) HousekeepingDiagnosticParameter = 0.5; and
- 3) FirePixel = 0.78.

The process of defuzzification is to convert the fuzzy set to a numeric value; i.e., the linguistic variable representing the output variable shall be converted to a numeric value [35]. The most common methods for the process of defuzzification of a fuzzy set in a discrete set are: the centroid method, the center of maximum method, and the central maximum average method [36]. The defuzzification method used for the proposed algorithm here is the centroid method.

## V. RESULTS

Simulations were performed with a database consisting of 80 sample images, provided by INPE. The images are from the same area and are related to the Amazon forest arc of deforestation region, acquired on

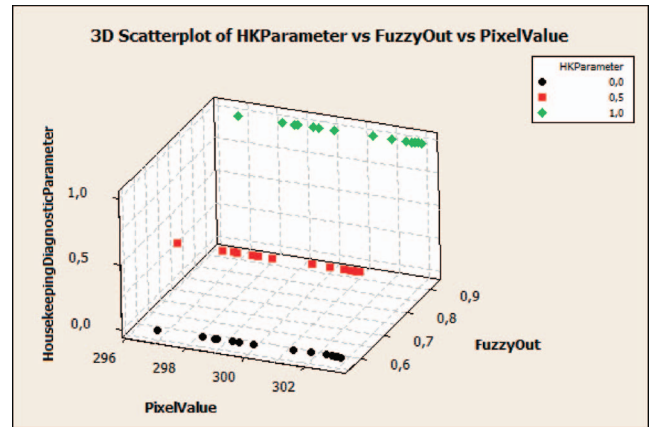


Fig. 6. Scatterplot of HousekeepingDiagnosticParameter versus PixelValue versus FuzzyOutput parameters.

TABLE III  
Simulations of HousekeepingDiagnosticParameter, as a Categorical Variable, Varying from 0 to 1

| PV    | HK | FO    | PV    | HK  | FO   | PV    | HK | FO     |
|-------|----|-------|-------|-----|------|-------|----|--------|
| 298.9 | 0  | 0.559 | 298.9 | 0.5 | 0.65 | 298.9 | 1  | 267.55 |
| 296.9 | 0  | 0.556 | 296.9 | 0.5 | 0.65 | 296.9 | 1  | 267.65 |
| 298.4 | 0  | 0.558 | 298.4 | 0.5 | 0.65 | 298.4 | 1  | 267.35 |
| 299.4 | 0  | 0.559 | 299.4 | 0.5 | 0.65 | 299.4 | 1  | 267.35 |
| 298.9 | 0  | 0.559 | 298.9 | 0.5 | 0.65 | 298.9 | 1  | 267.25 |
| 298.8 | 0  | 0.559 | 298.8 | 0.5 | 0.65 | 298.8 | 1  | 267.15 |
| 300.1 | 0  | 0.56  | 300.1 | 0.5 | 0.65 | 300.1 | 1  | 267.05 |
| 300.1 | 0  | 0.56  | 300.1 | 0.5 | 0.65 | 300.1 | 1  | 267.05 |
| 299.6 | 0  | 0.56  | 299.6 | 0.5 | 0.65 | 299.6 | 1  | 267.15 |
| 299.6 | 0  | 0.56  | 299.6 | 0.5 | 0.65 | 299.6 | 1  | 267.05 |
| 302.7 | 0  | 0.564 | 302.7 | 0.5 | 0.65 | 302.7 | 1  | 266.75 |
| 302.7 | 0  | 0.564 | 302.7 | 0.5 | 0.65 | 302.7 | 1  | 266.65 |
| 301.4 | 0  | 0.562 | 301.4 | 0.5 | 0.65 | 301.4 | 1  | 266.85 |
| 302   | 0  | 0.563 | 302   | 0.5 | 0.65 | 302   | 1  | 266.95 |
| 302.5 | 0  | 0.564 | 302.5 | 0.5 | 0.65 | 302.5 | 1  | 266.95 |
| 302.7 | 0  | 0.564 | 302.7 | 0.5 | 0.65 | 302.7 | 1  | 266.85 |
| 302.9 | 0  | 0.564 | 302.9 | 0.5 | 0.65 | 302.9 | 1  | 266.65 |
| 303   | 0  | 0.564 | 303   | 0.5 | 0.65 | 303   | 1  | 266.55 |
| 302.8 | 0  | 0.564 | 302.8 | 0.5 | 0.65 | 302.8 | 1  | 266.45 |
| 298.9 | 0  | 0.559 | 298.9 | 0.5 | 0.65 | 298.9 | 1  | 266.45 |
| 296.9 | 0  | 0.556 | 296.9 | 0.5 | 0.65 | 296.9 | 1  | 266.45 |

different days and in different months in 2013. This area shows an increase of fires during the months from June to August, as this is the winter period in which droughts mostly occur in Brazil. According to simulated analysis of the fuzzy system presented, results show that an optimization is done under the Setzer's algorithm to sustain an onboard satellite algorithm that is able to deal with the onboard environment. The proposed algorithm shows an improvement, when considering the parameters that were not considered in previous studies for the onboard processing.

Fig. 6 presents the categorical classification of the PixelValue and the HousekeepingDiagnosticParameter corresponding to their fuzzy outputs. As can be noticed, fuzzy outputs are sensitive to HousekeepingDiagnosticParameter variations, and correct

TABLE IV  
Samples of Each Channel of AVHRR/NOAA Sensor

| Image    | Description   | Fuzzy | INPE |
|----------|---|-------|------|
| Image_1  | 2013-08-27 12:42:22,NOAA-16N,Pium,TO,Parna do Araguaia              | 18    | 10   |
| Image_2  | 2013-08-28 12:30:11,NOAA-16N,Pium,TO,Parna do Araguaia              | 24    | 22   |
| Image_3  | 2013-08-29 12:18:17,NOAA-16N,Pium,TO,Parna do Araguaia              | 16    | 10   |
| Image_4  | 2013-09-05 12:33:10,NOAA-16N,Pium,TO,Parna do Araguaia              | 4     | 1    |
| Image_5  | 2013-09-13 12:37:49,NOAA-16N,Lagoa da Confusão,TO,Parna do Araguaia | 9     | 12   |
| Image_6  | 2013-09-14 12:24:05,NOAA-16N,Pium,TO,Parna do Araguaia              | 19    | 25   |
| Image_7  | 2013-09-14 12:24:05,NOAA-16N,Lagoa da Confusão,TO,Parna do Araguaia | 21    | 17   |
| Image_8  | 2013-09-15 12:13:05,NOAA-16N,Pium,TO,Parna do Araguaia              | 18    | 16   |
| Image_9  | 2013-09-16 12:00:33,NOAA-16N,Pium,TO,Parna do Araguaia              | 10    | 7    |
| Image_10 | 2013-09-23 12:16:01,NOAA-16N,Pium,TO,Parna do Araguaia              | 13    | 11   |
| Image_11 | 2013-09-23 12:16:01,NOAA-16N,Lagoa da Confusão,TO,Parna do Araguaia | 51    | 64   |
| Image_12 | 2013-10-25 12:26:22,NOAA-16N,Lagoa da Confusão,TO,Parna do Araguaia | 6     | 4    |
| Image_13 | 2013-10-26 12:14:59,NOAA-16N,Lagoa da Confusão,TO,Parna do Araguaia | 4     | 3    |

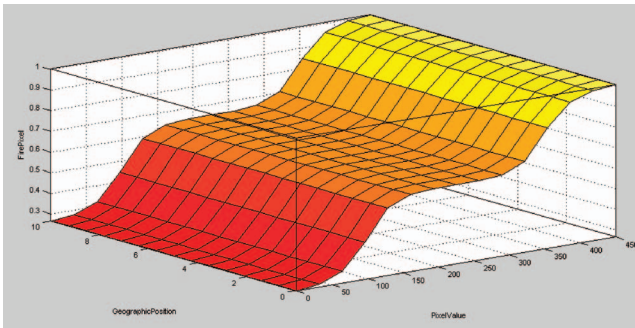


Fig. 7. Representation of surface area of plotted variables in proposed fuzzy logic system.

modeling of the real behavior of these variables for the PixelValue input variable.

As can be noticed from Table III, when HousekeepingDiagnosticParameter (HK) values vary from 0 to 1, the reliability of the PixelValue (PV) is compromised, and the fuzzy output (FO) decreases, as expected. Table IV presents a quantitative assessment of the improved hit rate using the fuzzy approach in comparison to INPE's current method for the classification of fire pixels. The use of fuzzy logic tends to increase the hit rate, basically because of the improvement of the thresholds gained through the Gaussian function for the pixel value.

Another improvement can be noticed when considering the Gaussian function to set the pixel value range for classification of the fire pixel. The thresholds are smoothed, and limits can better present accurate information obtained by researchers. The interaction between the variables shows the following behavior in Fig. 7.

It can be noted that the limits of the graph are the most critical areas for the analysis of burned or unburned areas in the pixel. However, considering the way that fuzzy logic has been structured, even in these regions, it is possible to obtain an output that best represents the behavior of the fire pixels from real data.

## VI. CONCLUSION

Considering the nature of the data in the onboard processing and the variables in this environment, fuzzy logic proved to be suitable for the process of recognizing patterns in data according to the results that were obtained in the tests. The noise of the images acquired by the sensor could be mitigated by the functions of each variable, and the outcome was optimized when compared to the algorithm currently used in ground stations.

This is due, primarily, to the way that the fuzzy system was implemented, taking into account variables that were not considered in the process described by Setzer et al. [25]. A fuzzy system can handle the errors produced by the lack of information of some variables and of the general condition of an embedded system, mainly due to factors that are intrinsic to the embedded system, which cannot be treated at the ground station for the actual pattern recognition process. The proposed fuzzy method for identification of active fires proved suitable for this proposed problem, since the results of the test showed an improvement in the hit rate compared with the same images analyzed by Setzer's algorithm.

## REFERENCES

- [1] Roy, D., Lewis, P., and Justice, C. Burned area mapping using multi-temporal moderate spatial resolution data—A bi-directional reflectance model-based expectation approach. *Remote Sensing of Environment*, **83**, 1–2 (Mar. 2002), 263–286.
- [2] Justice, C., Malingreau, J., and Setzer, A. W. Satellite remote sensing of fires: Potential and limitations. In *Fire in the Environment: The Ecological, Atmospheric, and Climatic Importance of Vegetation Fires*, P. J. Crutzen and J. G. Goldammer, Eds. New York: John Wiley, pp. 77–88.
- [3] Nepstad, D., Verissimo, A., Alencar, A., Nobre, C., Lima, E., Lefebvre, P., Schlesinger, P., Potter, C., Moutinho, P., Mendoza, E., Cochrane, M., and Brooks, V. Large-scale impoverishment of Amazonian forests by logging and fire. *Nature*, **398** (1999), 505–508.
- [4] Morelli, F., Libonati, R., and Setzer, A.

- Refinamento de um método de área queimada, e validação utilizando imagens CBERS no norte de Mato Grosso, Brasil. In *Anais XHI Simposio Brasileiro de Sensoriamento Remoto*, INPE, Florianopolis, Brazil, April 21–26, 2007, 4485–4492.
- [5] Chien, S., Doubleday, J., McLaren, D., Davies, A., Tran, D., Tanpipat, V., Akaakara, S., Ratanasuwana, A., and Mandl, D. Space-based sensorweb monitoring of wildfires in Thailand. In *Proceeding of the International Geoscience and Remote Sensing Symposium*, Vancouver, BC, Canada, Jul. 2011.
- [6] Ronquim, C. C. *Queimada na Colheita de Cana-de-Açúcar: Impactos Ambientais, Sociais e Econômicos*. Campinas, Brazil: Embrapa, 2010.
- [7] CPTEC/INPE. Fonte: Centro de Previsão e Estudos Climáticos, <http://www.cptec.inpe.br>. 2004. Last access May, 2013.
- [8] Malingreau, J., and Stephens, G. Remote-sensing of forest-fires—Kalimantan and north-Borneo in 1982–83. *Ambio*, **14**, 6 (1985), 314–321.
- [9] Matson, M., Stephens, G., and Robinson, J. Fire detection using data from the NOAA-N satellites. *International Journal of Remote Sensing*, **8**, 7 (1987), 961–970.
- [10] Langaas, S. A. A parameterised bispectral model for savanna fire detection using AVHRR night images. *International Journal of Remote Sensing*, **14**, 12 (1993), 2245–2262.
- [11] Kennedy, P. B. An improved approach to fire monitoring in West Africa using AVHRR data. *International Journal of Remote Sensing*, **15**, 11 (1994), 2235–2255.
- [12] Flannigan, M. D., and Vonder Haar, T. H. Forest fire monitoring using NOAA satellite AVHRR. *Canadian Journal of Forest Research*, **16** (1986), 975–982.
- [13] Kasischke, E. S., French, N. H. F., Harrell, P., Christensen, N. L., Jr., Ustin, S. L., and Barry, D. Monitoring of wildfires in boreal forests using large area AVHRR NDVI composite image data. *Remote Sensing of Environment*, **45**, 1 (1993), 61–71.
- [14] Lee, F. T. Improved detection of hot spots using the AVHRR 3.7  $\mu\text{m}$  channel. *Bulletin of the American Meteorological Society*, **71**, 12 (1990), 1722–1730.
- [15] Illera, P., Fernandez, A., and Casanova, J. L. Automatic algorithm for the detection and analysis of fires by means of NOAA AVHRR images. In *International Workshop on Satellite Technology and GIS for Mediterranean Forest Mapping and Fire Management*, November 4–6, 1994, 59–69.
- [16] Konecny, G. *Geoinformation—Remote Sensing, Photogrammetry and Geographic Information Systems*. London: CRC Press, 2002.
- [17] Figueiredo, D. *Conceitos Básicos de Sensoriamento Remoto*. Companhia Nacional de Abastecimento Eds. CONAB. Brasília - DF, (2005). Available at [http://72.14.205.104/search?q=cache:r9r3jyI5bKsJ:www.conab.gov.br/conabweb/download/SIGABRASIL/manuais/conceitos\\_sm.pdf+divino+figueiredo,+conceitod+basicos+sensoriamento+remoto&hl=pt-BR&ct=clnk&cd=1&gl=br](http://72.14.205.104/search?q=cache:r9r3jyI5bKsJ:www.conab.gov.br/conabweb/download/SIGABRASIL/manuais/conceitos_sm.pdf+divino+figueiredo,+conceitod+basicos+sensoriamento+remoto&hl=pt-BR&ct=clnk&cd=1&gl=br). Last access Jan., 2011.
- [18] Justice, C., and Dowty, P. *Technical Report of the IGBP-DIS Satellite Fire Detection Algorithm Workshop*. Greenbelt, MD: NASA/GSFC, 1993.
- [19] Skidmore, A. *Environmental Modelling and GIS and Remote Sensing*. London: Taylor & Francis Group, 2003.
- [20] Brieß, K., Bärwald, W., Gerlich, T., Jahn, H., Lura, F., and Studemund, H. The DLR small satellite mission BIRD. *Acta Astronautica*, **46**, 2–6 (2000), 111–120.
- [21] Oertel, D., Tank, V., Haschberger, P., Zhukov, B., Jahn, H., Briess, K., Knuth, R., Lorenz, E., and v. Schoenermark, M. FOCUS: Environmental disaster recognition system. In *ESA Symposium Proceedings on Space Station Utilisation*, ESOC, Darmstadt, Germany, Sept. 30–Oct. 2, 1996, 593–598.
- [22] Liu, J. W. *Real Time Systems*. Albuquerque, NM: Integre Technical Publishing Co., 2000.
- [23] Navulur, K. *Multispectral Image Analysis Using the Object-Oriented Paradigm*. Boca Raton, FL: CRC Press, 2006.
- [24] Lasaponara, R., and Lanorte, A. *Spectral Analysis of Burned Areas Observed in the Italian Peninsula by Using SPOT-Vegetation Data*. Potenza, Italy: Tito Scalo, 2003.
- [25] Setzer, A. W., Souza, P. A., and Morelli, F. Modificação do algoritmo de focos de queima AVHRR do INPE e sua avaliação com um método dinâmico. In *XVI Simpósio Brasileiro de Sensoriamento Remoto*, Foz do Iguaçu, PR, Brazil, April 13–18, 2013, 6.
- [26] Walsh, M. *Remote Sensing—Engineering and Design*. Engineer Manual. Washington, DC: Department of the Army, U.S. Army Corps of Engineers, 2003.
- [27] Campbell, J. B. *Introduction to Remote Sensing*. Vol. 5, R. H. Wynne, Ed. New York: Guilford, 2011.
- [28] Setzer, A. W., and Pereira, M. C. The operational detection of fires in Brazil with NOAA-AVHRR. In *Proceedings of the 24th International Symposium on Remote Sensing of Environment*, Rio de Janeiro, Brazil, May 27–31, 1991 76–77.
- [29] Schroeder, W. Comparação entre Métodos de Detecção de Focos de Calor para uma Região de Cerrado Usando Dados AVHRR/NOAA-14. In *Anais do XI Congresso Brasileiro de Meteorologia*, Rio de Janeiro, Brazil, 2000.
- [30] Gonzalez, R. C., and Woods, R. E. *Digital Image Processing* (3rd ed.). Prentice Hall, 2007. Pearson Education, 2002.
- [31] De Souza, A. L., Sismanoglu, A. R., Longo, M. K., Maurano, E. L., Recuero, S. F., Setzer, W. A., and Yoshida, M. C. Avanços no monitoramento de queimadas realizado no INPE. In *XIII Congresso Brasileiro de Meteorologia*, SBMET, Fortaleza, CE, Brazil, Aug. 29–Sept. 3, 2004. CD-ROM.
- [32] França, H. Identificação e mapeamento de cicatrizes de queimadas com imagens AVHRR/NOAA. In *Aplicações Ambientais Brasileiras dos Satélites NOAA e TIROS-N*, N. J. Ferreira, Ed. São Paulo: Oficina de Textos, 2004, 57–78.
- [33] Pereira, M. C. Detecção, monitoramento e análise de alguns efeitos ambientais de queimadas na Amazônia através da utilização de imagens dos satélites NOAA e LANDSAT e dados de aeronave. INPE-4503-TDL/326. São José dos Campos, Brazil: Instituto Nacional de Pesquisas Espaciais, 1987.

- [34] International Electrotechnical Commission, Technical Committee No. 65: Industrial-process Measurement and Control. Sub-committee 65B: Devices, Working Group 7: Programmable Controllers. Working Draft = IEC 61131-3, 2nd Ed. Programmable Controllers - Programming Languages. Geneva, Switzerland, Jan. 1, 1997.
- [35] Badiru, A. B., and Cheung, J. *Fuzzy Engineering Expert Systems with Neural Network Applications*. New York: Wiley, 2002.
- [36] Chen, W.-K. *Linear Networks and Systems*. Belmont, CA: Wadsworth, 1993, pp. 123–135.
- [37] Sá, J. P. *Pattern Recognition—Concepts, Methods and Applications*. Berlin, Heidelberg: Springer, 2001.
- [38] Escorial, D., Tourne, I., Reina, F. FUEGO: A dedicated constellation of small satellites to detect and monitor forest fires. In *Proc. of the 3rd IAA Symposium on Small Satellites for Earth Observation*, Berlin, Germany, 2001.



**B. E. Z. Leal** received the B.S. degree in computer science from Pontifical Catholic University of Sao Paulo, Sao Paulo, Brazil, in 2007, and the M.S. degree in computer engineering from University of São Paulo, Sao Paulo, Brazil, in 2010. She is currently pursuing the Ph.D. degree in computer engineering at University of Sao Paulo, Polytechnic School in 2016.

From 2012 to present, she is a software developer analyst with the Brazilian National Institute of Space Research, São José dos Campos, Brazil. She worked with the On-Board Data Handling Team from INPE's Aerospace Electronics Division with software systems and simulations for satellite on-board data handling and is now working with the Earth System Science Center (CCST) team from INPE with the emission modeling framework. Her research interest includes the development of methods and algorithms related to pattern recognition and fuzzy logic.



**A. R. Hirakawa** was born in São Paulo, Brazil, on June 15, 1965. He received the B.S. and M.S. degrees in electrical engineering from the University of Sao Paulo, São Paulo, Brazil, in 1991 and 1992, respectively. He received his Ph.D. degree in 1997 from the Department of Electrical and Computer Engineering, Yokohama National University, Japan. Since 1998, he has been with the Escola Polytechnic of Sao Paulo University (EPUSP), where he is currently an assistant professor. His current research interests include robotics, computational and communication architectures, and algorithms for robot control.



**T. D. Pereira** received the bachelor of information systems degree, in 2006, from Minas Gerais State University, Brazil, and the M.Sc. degree in space engineering and technology–systems engineering from Brazilian National Institute for Space Research (INPE), São José dos Campos, Brazil, in 2012.

He worked at INPE's Image Processing Division, in 2007, and since 2008 has been working for the On-Board Data Handling Team from INPE's Aerospace Electronics Division with software systems and simulations for satellite on-board data handling. His main areas of interest are systems engineering, software engineering, and pattern recognition.